Microstructure and mechanical properties of gas metal arc welded AISI 430/AISI 304 dissimilar stainless steels butt joints

Microstructure and mechanical properties of gas metal arc welded AISI 430/AISI 304 dissimilar stainless steels butt joints

Hüseyin Tarık SERİNDAĞ[1] and Gürel ÇAM[2, *]

[1] Iskenderun Technical University, Faculty of Aeronautics and Astronautics, Department of Aerospace Engineering, 31200 İskenderun-Hatay, Turkey
[2] Iskenderun Technical University, Faculty of Engineering and Natural Sciences, Department of Mechanical Engineering, 31200 İskenderun-Hatay, Turkey.

E-mail: gurel.cam@iste.edu.tr

Abstract. Nowadays, there is an increasing demand for the use of joining dissimilar metals in various industrial applications owing to the economic benefits and better joint performance. Ferritic stainless steel grades is a good alternative for austenitic ones in several applications as they display higher ductility and strength as well as better corrosion resistance in chloride environments. However, the poor ductility and low impact toughness of ferritic stainless-steel welded joints limit their wide-spread application. Thus, the demand for joining dissimilar ferritic and austenitic stainless steels is ever increasing in several engineering applications in various industries such as nuclear power plants, coal fired boilers, automobile manufacturing industry, chemistry and petro-chemistry industries, etc. Therefore, successful joining of these two different types of stainless steel grades using conventional fusion welding methods is rather important. In this study, the weldability of AISI 430 ferritic and AISI 304 austenitic steel plates using gas metal arc welding and the effect of heat input on microstructure and the mechanical properties were investigated. For this purpose, AISI 430 and AISI 304 plates with a thickness of 5 mm were joined using different heat input values. The microstructures evolved in the weld region of the joints and their mechanical properties were determined by detailed optical microscopy investigations, micro-hardness measurements and tensile tests. Thus, the influence of the heat input on the weldability of these two different stainless-steel plates using gas metal arc welding was also studied.

1. Introduction

Ferritic stainless steels (FSS), such as AISI 430, have higher resistance to stress corrosion cracking in chloride and caustic environments than austenitic stainless steels (ASS). In addition to that they have the advantage of having low cost. Thus, it is widely used in a wide spectrum of applications ranging from household utensils to oil, gas, petrochemical, nuclear and power industries [1-11]. However, the poor HAZ toughness of ferritic stainless steels after welding limits their wide-spread application in critical situations [3]. This problem has been related to the evolution of coarse grains as well as the formation of brittle intergranular martensite along the ferrite grains in the heat affected zone (HAZ) of fusion welds [4].

Although the austenitic stainless steels exhibit much superiority weldability than the ferritic grades, they are prone to stress corrosion cracking in chloride and caustic environments and they have a higher cost. Thus, the joint between austenitic and ferritic stainless steels may be advantageous in many instances. The demand for dissimilar ferritic-austenitic stainless steels joints is in fact increasing day by

day in several industries such as automotive, nuclear, chemical, petrochemical, and power generation industries. However, there are several concerns about joining these two different stainless steels. First of them is the much higher thermal expansion coefficient (CTE) of austenitic steels than ferritic grades which could probably result in the cracking within the weld region [7]. Secondly, the formation of chromium-depleted zones may be encountered in the HAZ of austenitic stainless steels side. The last but not the least, the occurrence of reduced ductility (toughness) in the HAZ of ferritic steel due to grain coarsening and intergranular martensite along the ferrite grain boundaries. Moreover, although the ferritic steels contain only small amounts of carbon, chromium-depleted zones (i.e., carbide precipitation) may take place along the ferrite grain boundaries in HAZ in addition to the martensite formation. Carbide precipitation can make both steels sensitive to inter-crystalline corrosion in HAZs. These problems become more pronounced as the heat input increases during welding.

For instance, Hsieh *et al.* [9] investigated the microstructural changes in gas tungsten arc welded dissimilar AISI 304/AISI 430 stainless steels joints. They observed that massive δ-ferrite precipitated within the austenite phases and at the ferrite-austenite interfaces within the fusion zone (FZ) which increased the hardness. Thus, the hardness of FZ was higher than that of the both base metals (BMs). It was suggested that the use of Ni-based filler wires could improve the performance of dissimilar ferritic-austenitic joints significantly. However, Shojaati and Beidokhti [10] conducted a detailed study on the influence of filler composition on the properties of dissimilar stainless steel joints, using E310, E316L, E2209, and Ni-based one. They reported that a weld microstructure consisting of a Ni-Cr-Fe matrix and iron-based precipitates was obtained by using the Ni-based filler metal. In addition, the fusion line cracking also occurred in this specimen due to the formation of a thin layer of martensite. The increase in the amount of δ-ferrite in the microstructure resulted in an increase in the hardness of the FZ. On the other hand, they did not observe any carbide/nitride phases in the joints produced using E310, E316L and E2209 filler wires. As pointed out above, the use of lower heat input is also suggested to minimize the problems encountered and successfully join these dissimilar stainless steels. In this respect, Khan *et al.* [11] studied the influence of weld parameters on the microstructure and hardness of laser beam (LB) welded dissimilar AISI 304L/AISI 430 joints. They observed that a continuous martensitic layer along ferrite grain boundaries and intergranular carbides of $Cr_{23}C_6$ were formed in the FZ. Therefore, the hardness of FZ was higher than those of both BMs. Similarly, Sun [12] also investigated the weldability of dissimilar ferritic and austenitic steels by LB welding. They reported that LB welding with nickel-based filler wire can be a potential process. However, they also pointed out that further data is still needed for ensuring the quality of the joints.

Another way of using low heat input is the employment of solid-state welding techniques. Thus, friction stir welding (FSW), a solid state welding technique used in joining of Al-alloys [13-18] as well as Cu-alloys [19-21] and Pb [22], offers a potential to join steels including stainless steels [23,24]. In addition to FSW, the low heat input CMT arc welding method [14,25] and power beam welding techniques such as laser beam welding [26-29] can also use. Due to this fact, numerous studies have been conducted on FSW of steels including stainless steels in last 30 years [24, 25, 30-38]. However, wear of the stirring tool is still a problem to overcome in FSW of these high melting materials since a peak temperature during this process may reach over 1000 ^{o}C, and even the tools made of high temperature resistant materials may wear slowly over the time. Thus, there is definitely a need for further work on dissimilar joining of ferritic and austenitic stainless steels.

In this study, the weldability of dissimilar AISI 430/AISI 304 stainless steel plates, and the influence of heat input applied to the plates during welding on the microstructural evolution in the joint area and on joint properties were investigated. For this purpose, AISI 430 and AISI 304 plates with a thickness of 5 mm were welded by gas metal arc welding (GMAW) using a filler wire of 308 with a diameter of 1.2 mm. Detailed microstructural investigations were carried out for microstructural characterization of the joints obtained. Additionally, detailed microhardness measurements across the joint area were conducted in addition to the mechanical tests (namely tensile and bend testing) in order to determine the joint properties. It was also evaluated that how the microstructural evolution, taking place in the weld region, and thus the joint performance of the joint was affected by heat input.

2. Materials and methods

AISI 430 grade ferritic stainless steel and AISI 304 grade austenitic stainless-steel plates both with a thickness of 5 mm were used in this study. They were supplied in the form of large plates with the sizes of 1500x1000x5 mm. Table 1 gives the chemical compositions and mechanical properties of both base plates, respectively.

In order to carry out this study, plates measuring 250x190 were cut. Before the welding process, the surfaces of the plates to be welded were cleaned with metal brush and the welding grooves were opened as shown in Figure 1. These plates were then joined by the GMAW method in two passes by feeding E307 filler wire at a rate of 17.5 mm/min. The parameters used for welding processes are given in Table 2. As can be understood from this table, two different heat inputs were applied to the weld region to evaluate the effect of the heat input on the weld behaviour.

Table 1. Chemical composition of AISI 304 grade austenitic steel plates used in this study.

	Chemical Composition (wt. %)									
Specimen	C	Si	Mn	P	S	Cr	Ni	N	Mo	Cu
Base Material (AISI 304)	0,019	0,42	1,56	0,035	0,002	18,2	8,1	0,053	--	--
Base Material (AISI 430)	0,037	0,38	0,50	0,031	0,002	16,16	0,27	0,033	0,01	0,20
Filler Material (ER307)	0,075	0,790	7,10	0,009	0,020	19,075	9,010	----	0,005	0,070

Table 2. The weld parameters employed in welding trials (the same weld parameters were used in each pass in both welding trials).

Weld Trial	Current (A)	Voltage (V)	Traverse speed (mm/s)	Wire feed rate (mm/s)	Shielding gas
Low Heat Input	ave. 385	28	4,5	17,5	Argon (99,95%)
High Heat Input	ave. 465	27	4,0	17,5	Argon (99,95%)

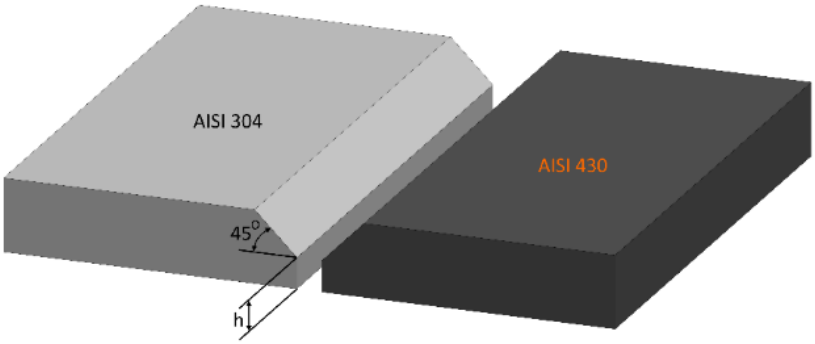

Figure 1. Preparation of the plates for welding trials.

After the welding trials, one metallography specimen, two bending specimens and four tensile specimens were prepared from each welded plate in order to demonstrate the influence of process parameters on the welding performance. In addition, in order to compare the mechanical properties of both joints with two base materials, four tensile specimens were also extracted from each base plate.

The metallography specimens cut from the joints produced were first ground and then polished before etching. Etching was carried out for about 20 seconds using 50 ml HCl and 150 ml HNO_3 solution. After etching, a detailed optical microscopy and extensive hardness measurements were performed on the metallography specimens. Hardness measurements were carried out for along three different lines (see Figure 2) on each specimen which in the center, 1 mm below the top and 1mm above the root using a load of 500 g.

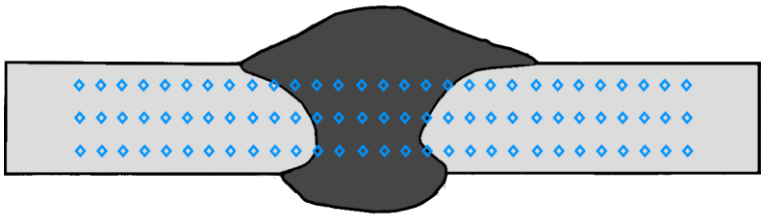

Figure 2. Schematic showing the conduction of microhardness measurements on each joint along three lines across the weld region, one being almost in the center, the other two lines lying 1 mm from the surface and root of the joints.

Tensile specimens prepared from both BMs and two welded joints using different heat input values were subjected to tensile tests at a loading rate of 15 mm/s and the mechanical performance values of the welded plates were determined. In addition, two bending specimens were prepared for each welded plate and subjected to bending test to investigate whether cracking occurs or not in weld region. In addition, the effect of heat input applied to the weld region on the microstructural changes taking place in fusion zone and HAZ and thus on weld performance was also evaluated.

3. Results and discussions

3.1. Microstructural aspects

Figure 3 gives the microstructures of the base metals used in this study, namely AISI 430 and AISI 304, respectively. As seen from Figure 3(a), ferritic stainless-steel base metal microstructure consists of a fully ferritic microstructure containing carbides evenly distributed within the grains as well as along the grain boundaries whereas austenitic stainless-steel base plate displays a single-phase microstructure consisting of austenite grains (Figure 3(b)). Figures 4 and 5 give macrographs and micrographs illustrating the weld cross-sections of the joints and the microstructures observed in base plate, FZ and HAZ of the joints produced using low and high heat inputs. Both joints exhibited similar microstructural evolutions within the weld region. A fine dendritic structure is observed in the FZ of both joints. However, the grain size of the dendrites is slightly coarser in the higher heat input joint due to the higher temperatures generated during welding.

Moreover, a crack was observed within the FZ of lower heat input joint neighboring the HAZ at the ferritic steel side whereas no weld defect was present in the weld region of the higher input joint (Figure 4). The reason for this cracking is much higher thermal expansion coefficient (CTE) of austenitic steels than ferritic grades as pointed out by [7]. Moreover, the formation of martensite within FZ and the fast cooling after the welding in the lower heat input joint may also lead to cracking. Shojaati and Beidokhti [10] also observed the fusion line cracking in the dissimilar stainless steel joints produced using a Ni-based filler metal. They attributed this to the formation of thin layer of martensite and the increased hardness of the FZ due to a high amount of δ-ferrite in the microstructure.

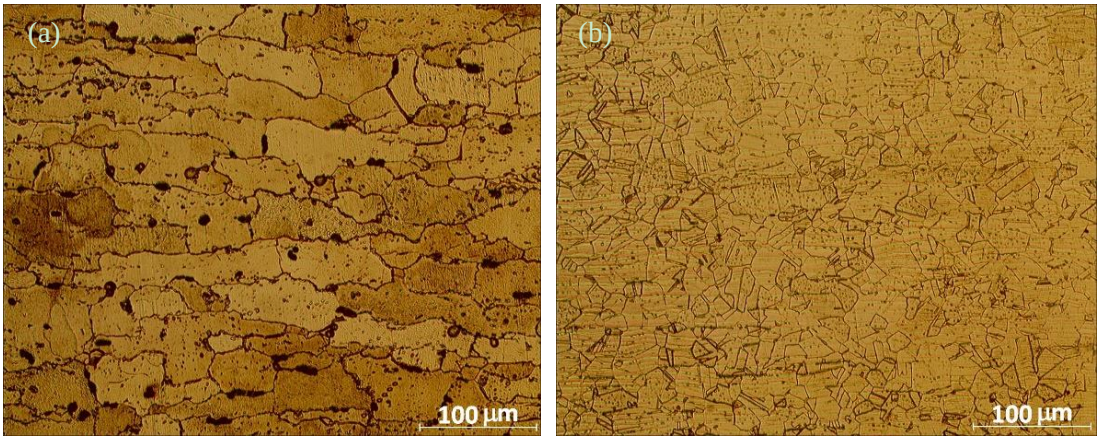

Figure 3. The micrograph illustrating the microstructure of the base plates: (a) AISI 430 and (b) AISI 304.

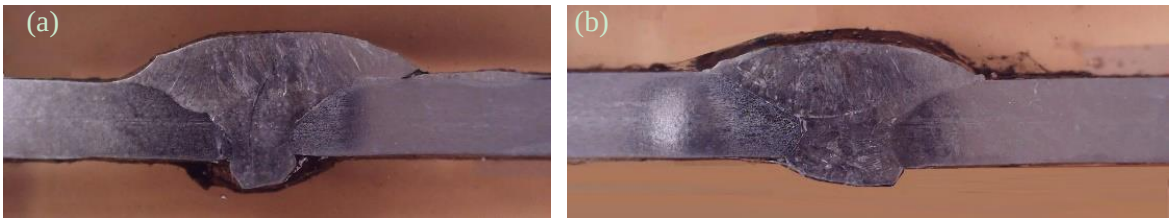

Figure 4. The macrographs illustrating the weld cross-sections of the joints produced: (a) the lower heat input joint and (b) the higher heat input joint.

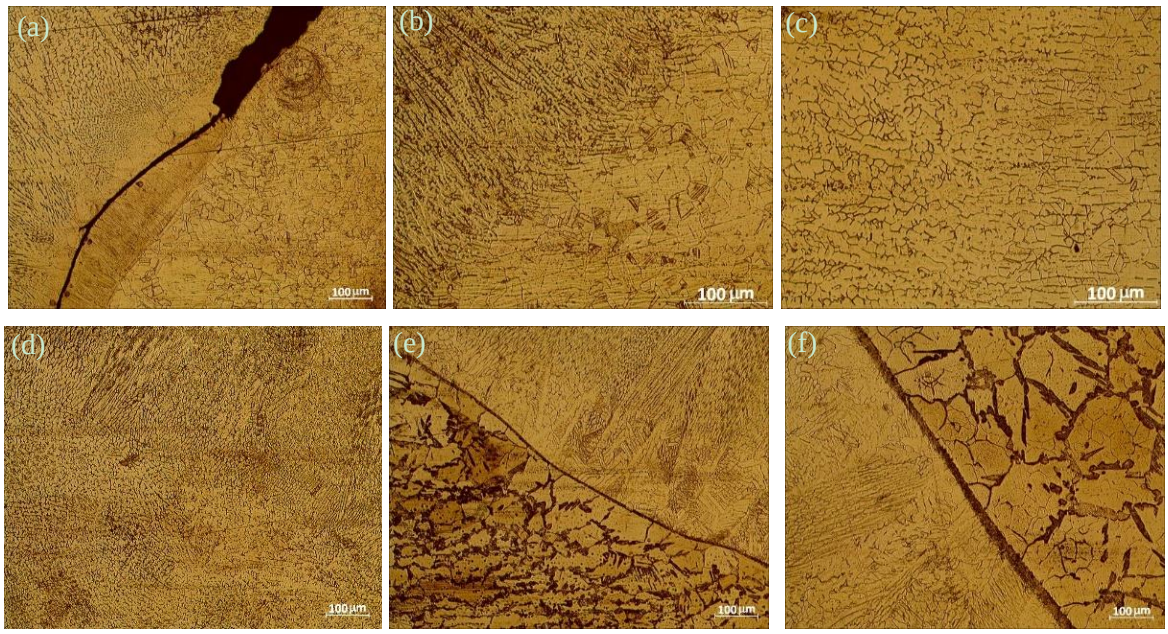

Figure 5. The micrographs illustrating the microstructures of: (a) cracking in the FZ of the lower heat input joint next to the A-HAZ, (b) A-HAZ of the lower heat input joint, (c) A-HAZ of the higher heat input joint, (d) FZ of the lower heat input joint, (e) F-HAZ of the lower heat input joint, and (f) F-HAZ of the higher heat input joint.

Furthermore, there is a clear difference between the microstructures evolving in the HAZs of both joints at the austenitic steel side (A-HAZs). As seen from Figure 5d, there are chromium carbide precipitates within the A-HAZ of the higher heat input joint elongated in the cold rolling direction, whereas no indication of carbide precipitation is visible within the A-HAZ of the lower heat input joint (Figure 5(c)). Moreover, the fusion interface is more distinct in the lower heat input joint. On the other hand, a carbide precipitation along the fusion boundary (fusion line) at the HAZs on the ferritic side (F-HAZs) of both joints. However, the carbide layer along the fusion line is thicker in the higher heat input joint due to the higher heat input involved as clearly seen in Figures. 5(e) and (f). Moreover, the formation of martensites at ferrite grain boundaries (i.e., intergranular martensites) was observed in the HAZ both joints next to the fusion boundary at the ferritic steel side (F-HAZs) in addition to the coarsening of ferrite grains. However, the F-HAZs of the two joints displayed different microstructural evolution. The ferritic side HAZ (F-HAZ) of the lower heat input joint exhibited a finer grained microstructure compared to that of the higher heat input joint. The reason for the formation of larger grains within the F-HAZ of the higher heat input joints is clearly the higher temperatures experienced by the plates during welding. On the other hand, both joints displayed a similar F-HAZ regions consisting of coarse grained HAZ (CGHAZ) and fine grained HAZ (FGHAZ) sections which were also reported by many other researchers [3, 39, 40].

3.2. Mechanical properties

Figure 6 gives the hardness profiles obtained from the microhardness measurements conducted along three lines across the joints produced using low and high heat inputs, respectively, showing the hardness variations across the joints. As clearly seen from these hardness profiles both joints exhibited similar hardness values across the weld region. There is a clear hardness increase at the F-HAZ of both joints due to the formation of intergranular martensites as well as the growth of ferrite grains in this region. However, as seen from Figure 6 the F-HAZ region of the higher heat input joint is wider than that of the lower heat input joint, indicating that the higher heat input widens the width of F-HAZ region.

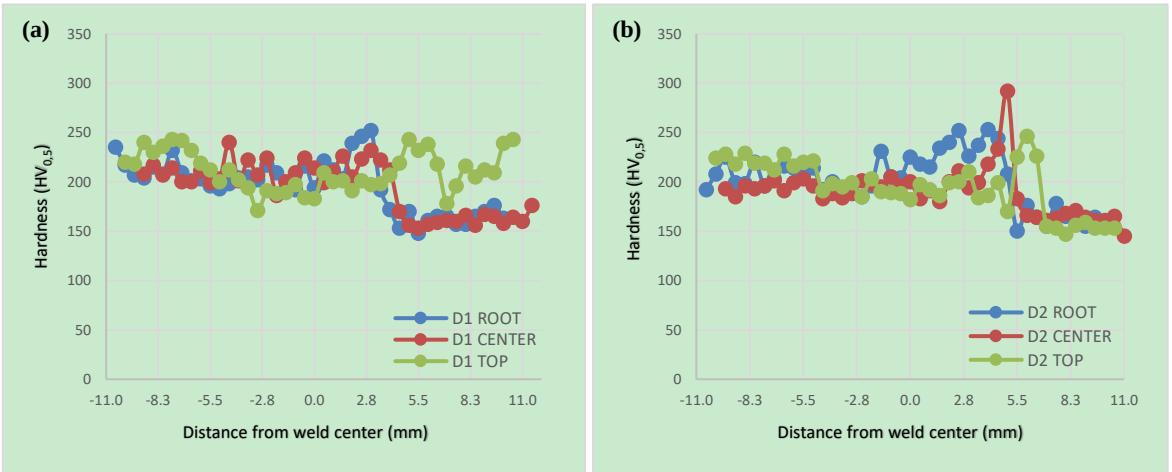

Figure 6. Hardness variation across the joints: (a) the lower heat input joint and (b) the higher heat input joint.

The results of all the tensile tests performed are summarized in Table 3. Moreover, Figure 7 compares the stress-strain curves obtained from BMs and the joints. The transverse tensile specimens extracted from both welded joints showed good tensile strength values similar to those of the lower strength AISI 430 base plate. Thus, the tensile strength performance of both joints was found to be about 100%.

Table 3. Tensile test results.

Specimen	**$R_{P0.2}$** (MPa)	**R_m** (MPa)	**Elongation** (%)	**Strength Performance** (%)	**Ductility Performance** (%)	**Failure Location**
AISI 430 BM	396, 392, 395 **(394)**	506,501,504 **(504)**	21, 25, 22 **(23)**	--	--	--
AISI 304 BM	366, 358, 359 **(361)**	643,631,633 **(636)**	48, 48, 49 **(48)**	--	--	--
Low Heat Input Joint	357, 369, 351, 362 **(360)**	510,514,500, 508 **(508)**	14,14,14,15 **(14.3)**	101[1] 80[2]	62[1] 30[2]	FGHAZ/BM transition zone
High Heat Input Joint	358, 341, 348, 324 **(343)**	498,495,504, 497 **(499)**	13,13,13,13 **(13)**	99[1] 78[2]	57[1] 27[2]	FGHAZ/BM transition zone

Notes: (Average values are given bold in parenthesis; BM: Base metal; FGAZ: Fine grained HAZ)
([1] Strength and ductility performance with respect to the lower strength base plate AISI 430 and [2] Strength and ductility performance with respect to the higher strength base plate AISI 304)

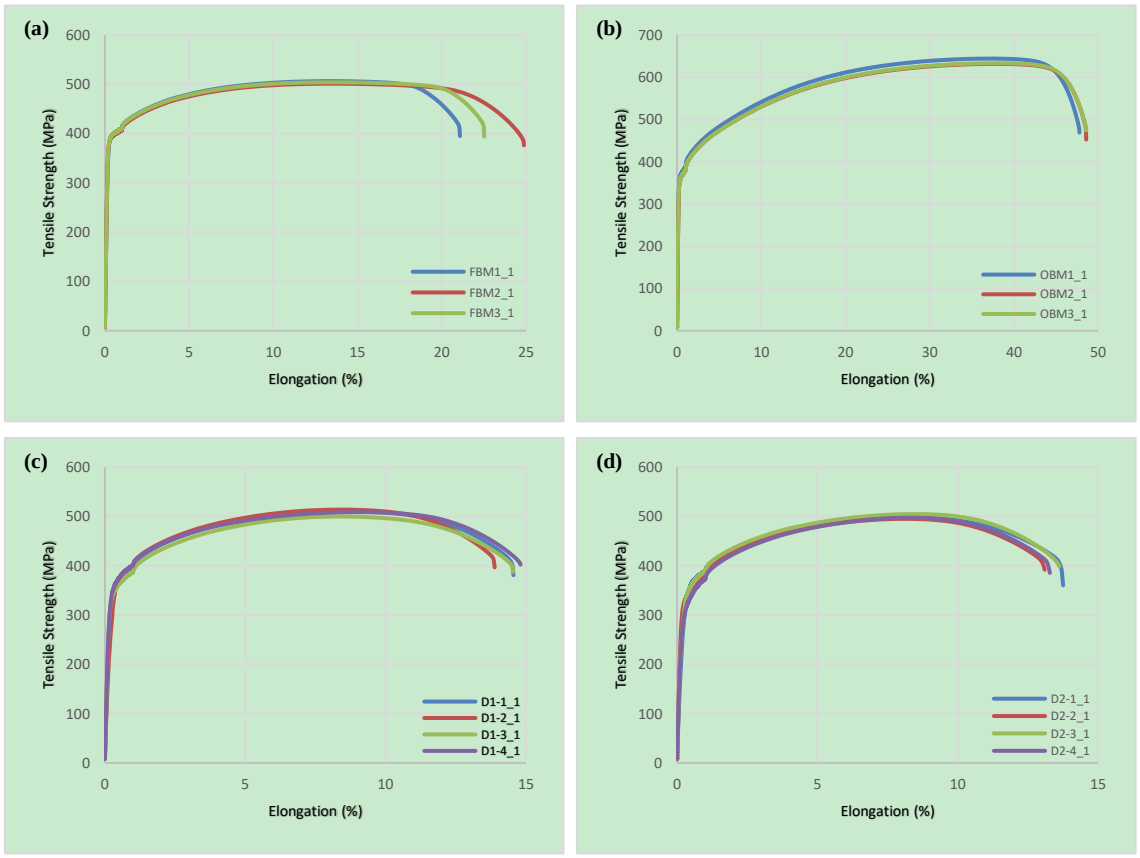

Figure 7. Stress-elongation (%) curves of: (a) the base plate AISI 430 steel, (b) the base plate AISI 304 steel (c) lower heat input joint, and (d) higher heat input joint.

On the other hand, both joints displayed lower ductility; i.e. about 14%, than that of the lower ductility AISI 430 base plate, i.e. 23%. The decrease in the elongation is slightly higher in the higher heat input joint as seen in Figure 7(c) and (d). This low ductility exhibited is not surprising since there

is a strength overmatching in both joints as seen from the hardness profiles. Thus, the higher strength weld region stays in the elastic region as well as the higher strength AISI 304 steel side (which forms almost half of the gauge length, l0) and only lower strength AISI 430 steel part of the gauge length underwent plastic deformation and contributed to the total elongation. Thus, both joints displayed low ductility values due to the confined plasticity. Similarly, low elongation values were also reported for inhomogeneous welded joints in the literature, namely strength overmatched laser beam welded steels [26, 41], strength undermatching Al-alloys joints [42-47] and bi-metallic joints showing confined plasticity [48,49].

Moreover, all the specimens extracted from both joints failed in the lower strength AISI 430 base plate away from weld region (in the transition region between FGHAZ and F-BM), as shown in Figure 8, although the lower heat input joint displayed a crack within the weld region next to the A-HAZ (Figure 5a). Even the presence of the crack did not change the fracture location, due to the strength overmatching nature of the weld region. This can be attributed to shielding effect of the overmatched weld zone and thus extensive plastic deformation developing at the lower strength AISI 430 ferritic stainless-steel side of the specimen. This shielding effect was also reported in the literature for laser beam welded dissimilar steel joints containing solidification cracks within fusion zone (FZ) [26,41].

Similar to tensile test, no effect of the heat input was observed on the joint behavior in bend testing. No cracking occurred in both surface and root bend specimens extracted from both joints as shown in Figure 9. The heat input difference used in this study apparently did not have any diminishing effect on the weld performance in spite of the existence of a crack in the FZ of the lower heat input joint next to the A-HAZ of the joint as well as intergranular martensite, grain coarsening were observed in the HAZ regions in addition to the carbide precipitation along the fusion boundary at the F-HAZ sides of both joints. These results indicate that the existence of crack in the fusion zone does not lead to failure in lower heat input joint, in other words the crack is shielded in bend testing in both surface and root bend configurations as the case in static transverse tensile testing.

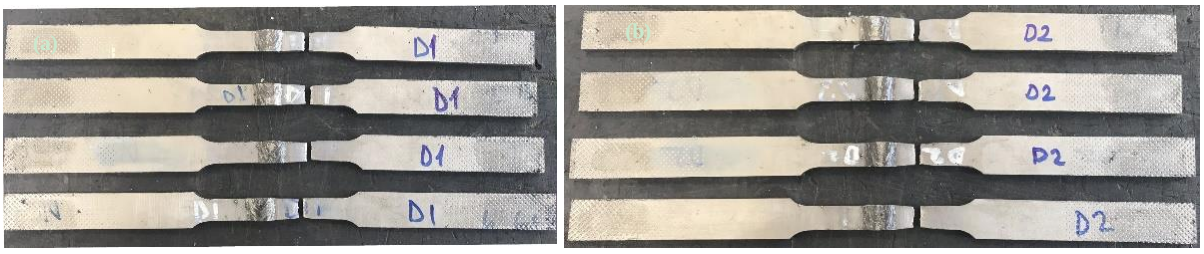

Figure 8. Macrographs showing the failure locations in the tensile test specimens extracted from: (a) lower heat input joint and (b) higher heat input joint.

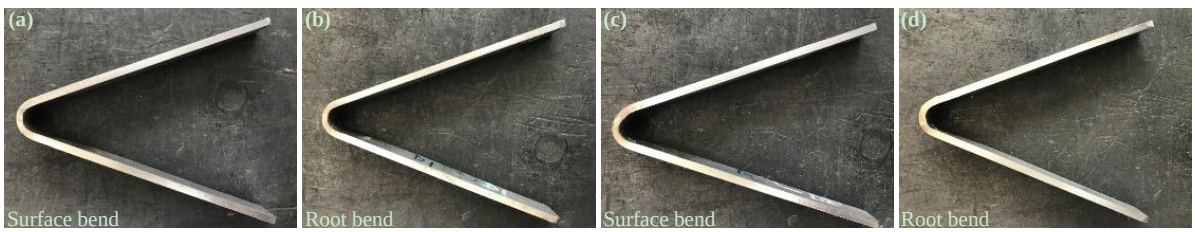

Figure 9. Macrographs showing the surface and root bend specimens extracted from: (a) lower heat input joint and (b) higher heat input joint. Note that no cracking occurred in any of the specimens.

4. Conclusions

The weldability of dissimilar AISI 430 / AISI 304 plates (both being 5 mm thick) by GMAW welded using a filler wire of 307 with a diameter of 1.2 mm has been studied. Furthermore, the influence of heat input on the microstructural evolution in the joint area and thus on joint properties of these dissimilar joints was investigated. The following conclusions were withdrawn from this study:

- Dissimilar AISI 430 / AISI 304 plates were defect-free welded in two passes by GMAW process. However, it was observed that cracking occurred in lower heat input joint due to higher thermal expansion coefficient (CTE) of austenitic steel than the ferritic grade. Thus, the welding conditions play a significant role in obtaining sound joint in this dissimilar stainless steel combination.
- A fine dendritic microstructure was evolved in the fusion zone of both joints, although the grain size of the dendrites was slightly finer in the lower heat input joint.
- Two distinct HAZ regions were formed in the ferritic base plate side (F-HAZs) of both joints namely coarse grained HAZ (CGHAZ) and fine grained HAZ (FGHAZ) regions. The formation of intergranular martensites and the growth of ferrite grains took place in the CGHAZ in addition to the carbide precipitation along the fusion boundary. However, no intergranular precipitates formed in the grains in the CGHAZ next to the fusion boundary.
- All the transverse tensile test specimens fractured in the transition zone between FGHAZ and the lower strength AISI 430 base plate far away from the FZ. Even the specimen extracted from the lower heat input joint containing crack in the FZ failed far away from the FZ due to shielding effect resulting from strength overmatching weld region.
- Both joints exhibited similar strength values to that of the lower strength base plate AISI 430, the strength performance of the joints being about 100%. However, the strength performance with respect to the higher strength base plate AISI 304 was much lower, about 80% for both joints. On the other hand, the ductility performance was lower, i.e. about 62% and 57% for the lower and higher heat input joint, respectively, due to both confined plasticity resulting from strength overmatching weld region and the higher strength AISI 304 part of the specimen.
- Both surface and root bend specimens extracted from both joints did not crack in bending test although a large crack exists in the FZ of the lower heat input joint. The results also indicate that the strength overmatching weld region shield the crack existing in FZ in both tensile and bending tests.

Acknowledgement

We would like to thank Mr. Tuğrul YAZGAN from NOKSEL Çelik Boru Sanayi A.Ş. (Noksel Steel Pipe Inc.), İskenderun-Hatay, Turkey, for his help in conduction of the metallography and mechanical tests. The authors also thank Hikmet Gizem SARSILMAZ from Kahraman-Sarsılmaz Machinery, İskenderun, for conducting welds.

References

[1] Ghosh N, Pal PK and Nandi G 2017 *Eng. Sci. Technol. an International Journal* **20**:1334–41.
[2] Mohandas T, Reddy MG and Naveed M 1999 *J. Mater. Process. Technol.* **94** 133-40.
[3] Lippold JC and Kotecki DJ 2005 *Welding Metallurgy and Weldability of Stainless Steels* (1st ed., Hoboken: John Wiley & Sons Inc.) p140.
[4] Pickering FB 1976 *Int. Met. Rev.* **21**: 227-68.
[5] Ghasemi R, Beidokhti B and Fazel-Najafabadi M 2018 *Arch. Metall. Mater.* **63**(1): 437-43.
[6] Aguilar S, Tabares R and Serna C 2013 *J. Mater. Phys. Chem.* **1**(4): 65-8.
[7] Arivarasu M, Kasinath D R, Natarajan A 2015 *Mater. Res.* **18**: 59-77.
[8] Dupont J N and Kusko C S 2007 *Weld. J.* **86**: 51-4.

[9] Hsieh C C, Lin D Y, Che M C and Wu W 2008 *Mater. Sci. Eng. A* **477**: 328-33.
[10] Shojaati M and Beidokhti B 2017 *Const. Build. Mater.* **147**: 608-15.
[11] Khan M, Romoli L, Fiaschi M, Dini G and Sarri F 2012 *J. Mater. Process. Technol.* **212**: 856-67.
[12] Sun Z 1996 *Int. J. Pres. Vessel Piping* **68**: 153-60.
[13] Kashaev N, Ventzke V and Çam G 2018 *J. Manuf. Process.* **36**: 571-600.
[14] Çam G and İpekoğlu G 2017 *Int. J. Adv. Manuf. Technol.* **91**(5-8): 1851-66.
[15] Çam G 2005 *Mühendis ve Makina* **46**(541): 30-9 (in Turkish).
[16] Von Strombeck A, Çam G, Dos Santos J F,Ventzke V and Koçak M 2001 *Proc. of the TMS Annual Meeting Aluminum, Automotive and Joining (New Orleans)* eds: S.K. Das, J.G. Kaufman, and T.J. Lienert (TMS, Warrendale, PA, USA) 249-64.
[17] Çam G *2001 Proc. of TMMOB Makina Mühendisleri Odası, Kaynak Teknolojisi III. Ulusal Kongresi* (İstanbul) 267-77 (in Turkish).
[18] İpekoğlu G, Gören Kıral B, Erim S and Çam 2012 *Mater. Tehnol.* **46**(6): 627-32.
[19] Küçükömeroğlu T, Şentürk E, Kara L, İpekoğlu G and Çam G 2016 *J. Mater. Eng. Perform.* **25 (1)**: 320-6.
[20] Çam G, Mistikoglu S and Pakdil M 2009 *Weld. J.* **88** (11): 225-32.
[21] Çam G, Serindağ H T, Çakan A, Mıstıkoğlu S and Yavuz H 2008 *Mat.-wiss. u. Werkstofftech.* **39**(6): 394-9.
[22] Günen A, Kanca E, Demir M, Çavdar F, Mistikoğlu S and Çam G 2018 *Indian J. Eng. Mater. Sci.***25**(1): 26-32.
[23] Çam G 2011 *Int. Mater. Rev.* **56(1)**: 1-48.
[24] Çam G, İpekoğlu G, Küçükömeroğlu T and Aktarer S M 2017 *J. Achievem. Mater. Manuf. Eng.* **80**(2): 65-85.
[25] Selvi S, Vishvaksenan A and Rajasekar E 2018 *Defence Technol.* **14**: 28-44.
[26] Çam G, Yeni Ç, Erim S, Ventzke V and Koçak M 1998 *Sci. Technol. Weld. Join.* **3**(4): 177-89.
[27] Dos Santos J, Çam G, Torster F, Insfran A, Riekehr S, Ventzke V and Koçak M 2000 *Weld. World* **44**(6): 42-64.
[28] Çam G, Koçak M and dos Santos J F 1999 *Weld. World* **43**(2): 13-26.
[29] Çam G, Ventzke V, dos Santos J F, Koçak M, Jennequin G, Gonthier-Maurin P, Penasa M and Rivezla C 1999 *Prakt. Metallogr.* **36**(2): 59-89.
[30] Küçükömeroğlu T, Aktarer S M, İpekoğlu G and Çam G 2019 *The 2nd International Conference on Material Strength and Applied Mechanics* (Kiev) IOP Conf. Series Mater. Sci. Eng. **629** 012010.
[31] İpekoğlu G, Küçükömeroğlu T, Aktarer S M, Sekban DM and Çam G 2019 *Mater. Res. Express* **6**(4): 046537.
[32] Küçükömeroğlu T, Aktarer SM, İpekoğlu G and Çam G 2018 *Mater. Testing* **60**(12): 1163-70.
[33] Küçükömeroğlu T, Aktarer SM, İpekoğlu G and Çam G 2018 *Int. J. Min. Met. Mater.* **25**(12): 1457-64.
[34] Cui L, Fujii H, Tsuji N and Nogi K 2007 *Scripta Mater.* **56**: 637-40.
[35] Azuma Y, Kameno Y and Takasugi T 2013 *Weld. Int.* **27**(12): 929-35.
[36] Ahn B W, Choi D H, Kim D J and Jung S B 2012 *Mater. Sci. Eng. A* **532**: 476-9.
[37] Lakshminarayanan A K and Balasubramanian V 2010 *Mater. Des.* **31**: 4592-4600.
[38] Heidarzadeh A, Mironov S, Kaibyshev R, Çam G, Simar A, Gerlich A, Khodabakhshi F, Mostafaei A, Field D P, Robson J D, Deschamps A and Withers P J 2020 *Progress in Materials Science* (DOI: https://doi.org/10.1016/j.pmatsci.2020.100752).
[39] Khorrami M S, Mostafaei M A, Pouraliakbar H and Kokabi A H 2014 *Mater. Sci. Eng. A* **608**: 35-45.
[40] Van Warmelo M, Nolan D and Norrish J 2007 *Mater. Sci. Eng. A* **464**: 157-69.
[41] Çam G, Erim S, Yeni Ç and Koçak M 1999 *Weld. J.* **78**(6): 193-201.
[42] Çam G, Ventzke V, dos Santos J F, Koçak M, Jennequin G and Gonthier-Maurin P 1999 *Sci. Technol. Weld. Join.* **4**(5): 317-23.

[43] İpekoğlu G, Erim S, Gören Kıral B and Çam G 2013 *Kovove Mater.* **51**(3): 155-63.
[44] Çam G, Güçlüer S, Çakan A and Serindağ H T 2009 *Mat.-wiss. u. Werkstofftech.* **40**(8): 638-42.
[45] Pakdil M, Çam G, Koçak M and Erim S 2011 *Mater. Sci. Eng. A* **528**(24): 7350-6.
[46] İpekoğlu G, Erim S and Çam G 2014 *Metall. Mater. Trans. A* **45A**(2): 864-77.
[47] İpekoğlu G, Erim S and Çam G 2014 *Int. J. Adv. Manuf. Technol.* **70**(1): 201-13.
[48] Koçak M, Pakdil M and Çam G 2002 *Sci. Technol. Weld. Join.* **7**(4): 187-96.
[49] Çam G, Koçak M, Dobi D, Heikinheimo L and Siren M 1997 *Sci. Technol. Weld. Join.* **2**(3): 95-101.